

Article

Selective CO Hydrogenation Over Bimetallic Co-Fe Catalysts for the Production of Light Paraffin Hydrocarbons (C₂–C₄): Effect of Space Velocity, Reaction Pressure and Temperature

Seong Bin Jo ^{1,†}, Tae Young Kim ^{2,†}, Chul Ho Lee ², Jin Hyeok Woo ², Ho Jin Chae ¹ , Suk-Hwan Kang ³, Joon Woo Kim ⁴, Soo Chool Lee ^{1,*} and Jae Chang Kim ^{2,*}

¹ Research Institute of Advanced Energy Technology, Kyungpook National University, Daegu 41566, Korea; santebin@knu.ac.kr (S.B.J.); hwman777@nate.com (H.J.C.)

² Department of Chemical Engineering, Kyungpook National University, Daegu 41566, Korea; tyoung0218@knu.ac.kr (T.Y.K.); cjfgh38@knu.ac.kr (C.H.L.); wjh8865@knu.ac.kr (J.H.W.)

³ Institute for Advanced Engineering, Yongin 41718, Korea; shkang@iae.re.kr

⁴ Research Institute of Industrial Science and Technology, Pohang 37673, Korea; realjoon@rist.re.kr

* Correspondence: soochool@knu.ac.kr (S.C.L.); kjchang@knu.ac.kr (J.C.K.); Tel.: +82-53-950-5622 (S.C.L. & J.C.K.)

† Seong Bin Jo and Tae young Kim contributed equally to this work.

Received: 6 August 2019; Accepted: 16 September 2019; Published: 19 September 2019



Abstract: Synthetic natural gas (SNG) using syngas from coal and biomass has attracted much attention as a potential substitute for fossil fuels because of environmental advantages. However, heating value of SNG is below the standard heating value for power generation (especially in South Korea and Japan). In this study, bimetallic Co-Fe catalyst was developed for the production of light paraffin hydrocarbons (C₂–C₄ as well as CH₄) for usage as mixing gases to improve the heating value of SNG. The catalytic performance was monitored by varying space velocity, reaction pressure and temperature. The CO conversion increases with decrease in space velocities, and with an increase in reaction pressure and temperature. CH₄ yield increases and C₂₊ yield decreases with increasing reaction temperature at all reaction pressure and space velocities. In addition, improved CH₄ yield at higher reaction pressure (20 bar) implies that higher reaction pressure is a favorable condition for secondary CO₂ methanation reaction. The bimetallic Co-Fe catalyst showed the best results with 99.7% CO conversion, 36.1% C₂–C₄ yield and 0.90 paraffin ratio at H₂/CO of 3.0, space velocity of 4000 mL/g/h, reaction pressure of 20 bar, and temperature of 350 °C.

Keywords: Synthetic natural gas (SNG); Cobalt; Iron; Fischer-Tropsch synthesis; C₂–C₄ hydrocarbons; paraffin ratio

1. Introduction

At present, the production of synthetic natural gas (SNG), mainly consisting of methane, has aroused extensive attention and been commercially produced from different starting materials, including coal and solid dry biomass (e.g., wood and straw) [1–5]. CH₄ via synthesis gas (syngas, CO + 3H₂) is an effective and environmentally friendly method, because it emits the smallest amount of CO₂ per energy unit among all fossil fuels. However, the heating value of CH₄ is typically below the standard heating value for power generation (especially in South Korea and Japan) [6–12]. For power generation, liquefied petroleum gas (LPG, C₃–C₄ hydrocarbons) must be added to SNG to enhance its heating value; however, the price of LPG is strongly correlated with that of oil. In principle,

synthetic light hydrocarbons (C_1 – C_4 ranges) via Fischer–Tropsch (FT) reaction could be added to SNG as a substitute for LPG by using the same syngas source (H_2/CO ratio = 3.0) for the SNG process. Furthermore, the gas products must maintain a high paraffin ratio, because olefins exhibit a low heating value, as well as being more susceptible to hydration with CH_4 and liquefaction than paraffins of the same carbon chain length under pipeline conditions ($-5\text{ }^\circ\text{C}$, 70 bar) [13]. Therefore, the FT product gas must have a high paraffin ratio in C_2 – C_4 ranges, as well as a high light hydrocarbon yield (CH_4 and C_2 – C_4) if it is to be used to replace LPG for power generation.

Inui et al. reported a “high calorific methanation” process using Co-Mn-Ru/ Al_2O_3 catalyst for the production of high-calorie gas comparable to natural gas with added C_2 – C_4 hydrocarbons [6]. The Co-Mn-Ru/ Al_2O_3 catalyst afforded high CO conversion (98.8%) and C_2 – C_4 selectivity (19.1%). Lee et al. elucidated the role of each component in the Co-based catalysts, and proposed the 10Co-6Mn-2.5Ru/ Al_2O_3 and 20Co-16Mn/ Al_2O_3 as optimum catalysts for high heating value of SNG [7]. They also developed Fe-Zn and Fe-Cu catalysts, and the Fe-based catalysts were evaluated after carburization and reduction pretreatment [8–10]. In an earlier report, bimetallic Co-Fe catalysts supported on γ - Al_2O_3 were developed for the production of light hydrocarbons (C_2 – C_4 ranges) at high CO conversion [11]. It was found that the reducibility of the iron phase was enhanced in the presence of cobalt, leading to enhanced catalytic activity. Of all catalysts, 5Co-15Fe/ γ - Al_2O_3 exhibited the highest C_2 – C_4 paraffin selectivity at high CO conversion. The high CO conversion and similar hydrocarbon distribution of 5Co-15Fe/ γ - Al_2O_3 compared to 20Fe/ γ - Al_2O_3 is due to improved iron reducibility. Moreover, the effects of the H_2/CO gas ratio and the reaction temperature on the catalytic performance over 5Co-15Fe/ γ - Al_2O_3 catalyst were investigated: the FT catalyst showed high paraffinic C_2 – C_4 selectivity and CO conversion at $H_2/CO = 3.0$, reaction temperature of $300\text{ }^\circ\text{C}$ and pressure of 10 bar; but this led to substantial byproduct formation, such as C_{5+} liquid and waxy hydrocarbons and CO_2 . Despite the high C_2 – C_4 yield, a considerable amount of byproducts (C_{5+} hydrocarbons and CO_2) need to be condensed or separated to be used as mixing gases in SNG for practical processing. To overcome this problem, hybrid catalysts (FT + cracking) in a double-layered bed reactor system were introduced to minimize C_{5+} and CO_2 [12]. The layer of cracking catalysts (SAPO-34 zeolite and Ni catalysts) was loaded underneath the FT catalyst (5Co-15Fe/ γ - Al_2O_3) layer in the double-layered bed reactor system. Compared with the FT catalyst in a single-layered bed reactor, cracking catalysts (SAPO-34 and Ni catalysts) convert C_{5+} hydrocarbons into light hydrocarbons (CH_4 and C_2 – C_4) in the double-layered bed reactor system. In addition, the Ni catalyst improved the CO conversion and reduced the CO_2 yield via methanation.

At present, few studies have made an effort to improve the heating value of SNG by producing paraffinic C_2 – C_4 hydrocarbons and minimizing byproducts (C_{5+} and CO_2). Although catalytic performance, including CO conversion and hydrocarbon distribution, is strongly dependent on the operation conditions such as space velocity, reaction pressure and temperature in the practical process, these effects were not investigated in detail. Herein, catalytic performance over bimetallic Co-Fe catalyst (5Co-15Fe/ γ - Al_2O_3) under different reaction conditions (SV, P and T) is evaluated to determine the optimum operating conditions for the production of high paraffinic C_2 – C_4 yield, as well as reduction of byproduct (C_{5+} and CO_2). In addition, characterization of the catalysts was performed using inductively coupled plasma optical emission spectroscopy (ICP-OES), X-ray diffraction (XRD) techniques and Brunauer-Emmett-Teller (BET) analysis.

2. Results

Table 1 shows the metal content and textural properties, such as BET surface area, pore volume, and average pore size, of support material (γ - Al_2O_3) and FT catalyst (5Co-15Fe/ γ - Al_2O_3). As listed in Table 1, the metal content in FT catalyst (5Co-15Fe/ γ - Al_2O_3) is 5.2 wt.% Co and 14.1 wt.% Fe, which is almost consistent with the intended metal loading. The γ - Al_2O_3 shows a BET surface area of $156.9\text{ m}^2/\text{g}$, pore volume of $0.23\text{ cm}^3/\text{g}$ and average pore size of 5.9 nm, and those values decreased after impregnation of γ - Al_2O_3 with cobalt and iron. In addition to γ - Al_2O_3 (JCPDS No.

10-0425), fresh 20Co/ γ -Al₂O₃ and 20Fe/ γ -Al₂O₃ catalysts showed Co₃O₄ phase (JCPDS No. 43-1003) and Fe₂O₃ phase (JCPDS No. 52-1449), respectively (Figure S1) [11]. However, the XRD peaks of Fe phase are very broad compared to those of Co₃O₄ phase, due to the high dispersion of iron phase on γ -alumina [11,12,14,15]. In the case of the bimetallic Co-Fe catalysts, the XRD peaks of Co₃O₄ decreased and those of Fe₂O₃ increased slightly with increasing iron-to-cobalt ratio. However, fresh 5Co-15Fe/ γ -Al₂O₃ showed XRD patterns of CoO (JCPDS No. 48-1719) and Fe₂O₃ phases, indicating the incorporation of Co into Fe₂O₃ after calcination, as shown in Figure 1 [11,12,14,15]. On the other hand, the reduced 5Co-15Fe/ γ -Al₂O₃ showed XRD peaks of Co metal (JCPDS No. 01-1259) and Fe metal (JCPDS No. 87-0722), respectively. The crystallite size of CoO phase is 4.7 nm, while that of Fe₂O₃ could not be calculated because of the too-broad peaks of Fe₂O₃, as mentioned above. In reduced states of the catalyst, crystallite sizes of the Fe metal are ~20 nm. Based on the H₂-TPR results, reduction temperatures of cobalt phase increased, and those of iron decreased with the increasing iron-to-cobalt ratio (Figure S2). Thus, it can be concluded that the incorporation of Co into the Fe₂O₃ phase results in a weaker interaction between iron and alumina, which enhance the reducibility of iron species and catalytic activity (Figure S3). Therefore, the 5Co-15Fe/ γ -Al₂O₃ catalyst was chosen as the catalyst with optimum mass ratio for the following studies.

Table 1. Characterization of γ -Al₂O₃ support material and FT catalyst (5Co-15Fe/ γ -Al₂O₃).

	Metal Content (wt.%) ^a		Textural Properties			Crystallite Size (nm) ^c			
	Co	Fe	BET Surface Area (m ² /g)	Pore Volume (cm ³ /g)	Average Pore Size (nm) ^b	Fresh		Reduced	
						CoO	Fe ₂ O ₃	Co ⁰	Fe ⁰
γ -Al ₂ O ₃	-	-	156.9	0.23	5.9	-	-	-	-
5Co-15Fe/ γ -Al ₂ O ₃	5.2	14.1	40.6	0.09	4.6	4.7	-	-	20

^a Metal contents were determined by ICP-OES. ^b Average pore size were measured following the Barrett-Joyner-Halenda (BJH) method. ^c Crystallite sizes of metal phase were calculated using the Scherer equation.

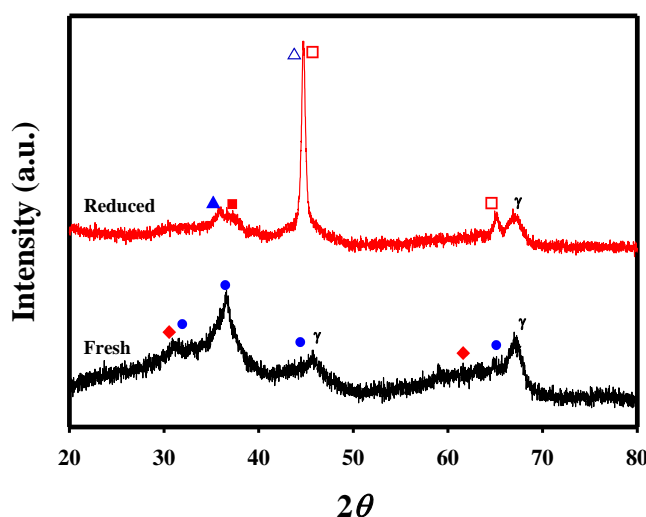


Figure 1. XRD patterns of the FT catalyst (5Co-15Fe/ γ -Al₂O₃) in fresh and reduced states; (●) Co₃O₄, (▲) CoO, (△) Co metal, (◆) Fe₂O₃, (■) Fe₃O₄, and (□) Fe metal.

Figure 2 shows the CO conversion of FT catalyst (5Co-15Fe/ γ -Al₂O₃) as a function of time on stream after reduction at 500 °C for 1 h under a 10% H₂/N₂ gas mixture. Activity tests were conducted under conditions of H₂/CO = 3.0 at different reaction parameters, such as space velocity, reaction pressure and temperature. Overall, CO conversion of the FT catalyst increased with the increase in reaction temperature. Under almost all operating conditions, the FT catalyst maintains its CO

conversion and yield of hydrocarbons. However, the CO conversion of the FT catalyst decreased below 10 bar, with a space velocity of 8000 mL/g/h, at 300 and 350 °C (Figure 2c). CO conversion decreased from 64.9 to 55.9% at 300 °C, and from 97.9 to 81.4% at 350 °C as the reaction progressed. It is well known that the deactivation of the catalysts in CO hydrogenation is due to several factors, including sintering, re-oxidation of active materials, poisoning, coke formation on the surface of active materials, etc., but its causes and effects are not elucidated in this paper. The deactivation of the FT catalysts was compensated by the high reaction temperature (Figure 2c) and pressure (Figure 2f), leading to an increase in CO conversion [16].

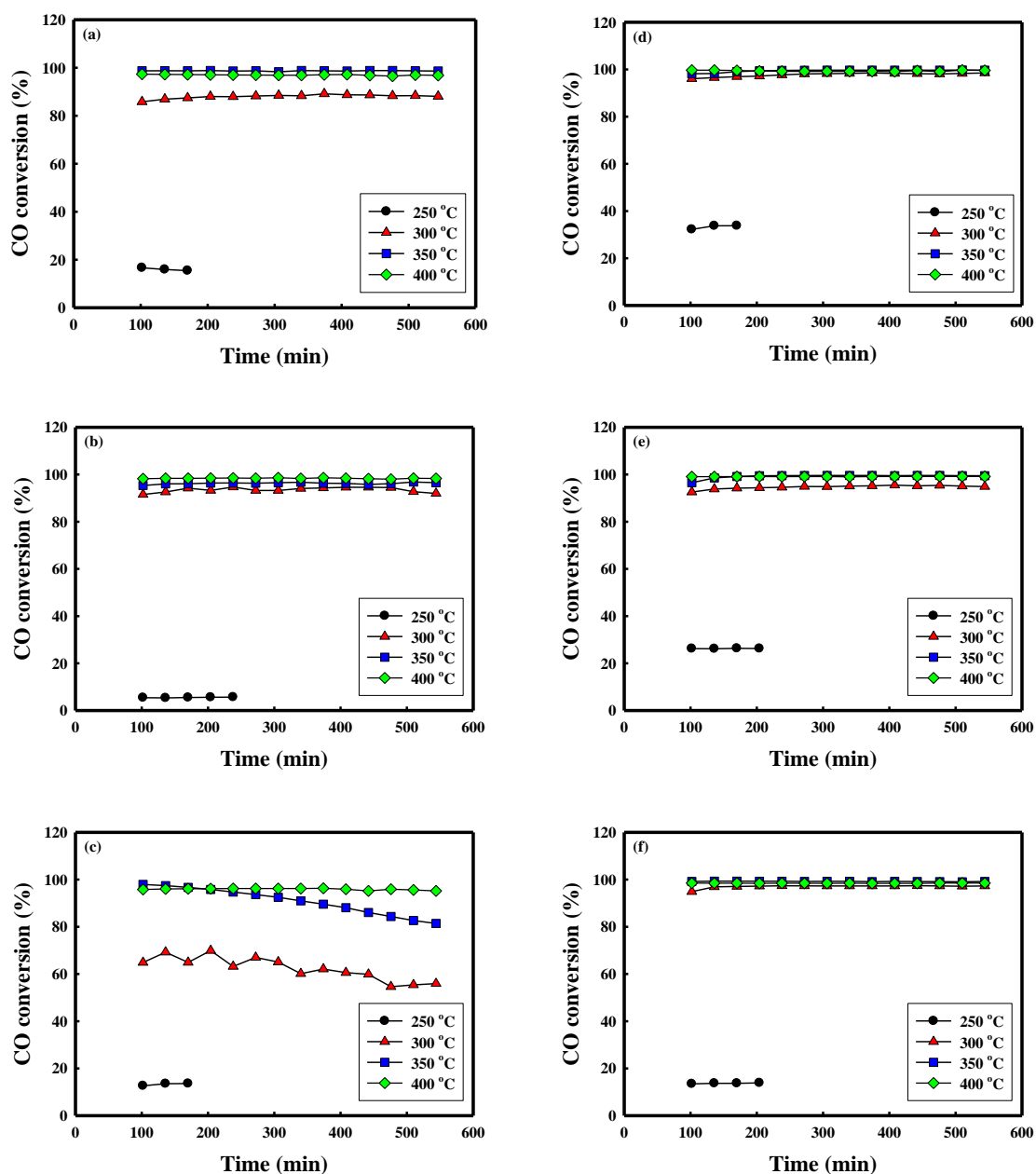


Figure 2. CO conversion of FT catalyst at different reaction temperature under 10 bar (left) and 20 bar (right) at space velocity of (a,d) 4000, (b,e) 6000, and (c,f) 8000 mL/g/h as a function of time on stream.

The results of the catalytic behavior, such as the initial CO conversion and initial hydrocarbon yield of the FT catalyst, are shown in Figures 3 and 4, and summarized in Table 2. Figure 3 shows the initial CO conversion of the FT catalyst as a function of reaction temperature. As shown in Figure 3, the initial

CO conversion of the catalyst increased dramatically to 300 °C, and then increased slightly above 350 °C at all pressures and space velocities. Furthermore, it was also found that the CO conversion increased with the increase in reaction pressure, and with the decrease in space velocity. At high temperature (≥ 300 °C), CO conversion appears to be largely independent of space velocity and reaction pressure. It was reported that CO conversion initially increased dramatically, and then decreased with increasing reaction temperatures (>400 °C) [17,18]. In addition, CO conversion increased with increase in reaction pressure and decrease in space velocity [18,19]. However, space velocity and reaction pressure have little effect on CO conversion, because high reaction temperature (≥ 300 °C) has a significant influence on CO conversion.

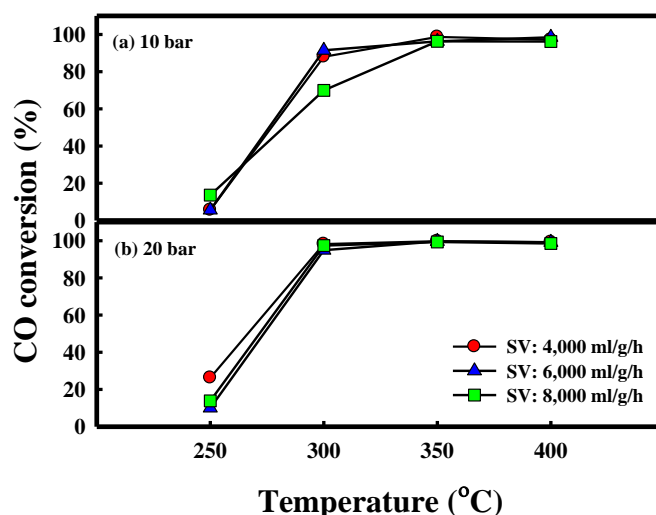


Figure 3. The initial CO conversion of the FT catalyst ($5\text{Co-15Fe}/\gamma\text{-Al}_2\text{O}_3$) under (a) 10 and (b) 20 bar at different space velocities as a function of reaction temperature.

Table 2. Summarization of catalytic performance over FT catalyst ($5\text{Co-15Fe}/\gamma\text{-Al}_2\text{O}_3$) at different space velocity, reaction pressure and temperature.

P (bar)	SV (ml/g/h)	T (°C)	Conversion			Yield (%)			$\frac{(\text{C}_2\text{-C}_4)}{(\text{C}_1\text{-C}_4)}$	P/(P+O)
			CO	H ₂	CH ₄	C ₂ -C ₄	C ₅₊	CO ₂		
10	4000	300	88.0 ± 1.2	43.1 ± 0.5	26.7 ± 0.9	26.9 ± 1.8	15.4 ± 0.3	19.1 ± 0.1	0.50	0.96
		350	98.7 ± 0.1	49.3 ± 0.2	31.7 ± 2.1	31.8 ± 0.6	13.9 ± 2.5	21.2 ± 0.2	0.50	0.89
		400	97.2 ± 0.2	51.7 ± 0.2	42.5 ± 1.5	23.5 ± 1.8	11.5 ± 0.5	19.7 ± 0.4	0.36	0.82
	6000	300	91.5 ± 1.0	38.2 ± 0.9	21.5 ± 0.7	25.8 ± 0.6	23.8 ± 1.6	20.4 ± 0.4	0.55	0.98
		350	96.4 ± 0.2	40.0 ± 0.8	32.3 ± 0.4	23.2 ± 0.3	14.3 ± 0.7	26.6 ± 0.2	0.42	0.91
		400	98.5 ± 0.0	47.6 ± 0.2	43.9 ± 0.5	19.1 ± 1.5	12.4 ± 2.1	23.0 ± 0.2	0.30	0.87
	8000	300	77.1 ± 15.1	35.8 ± 6.6	22.8 ± 1.1	22.2 ± 2.2	9.2 ± 3.2	15.7 ± 3.3	0.49	0.88
		350	96.3 ± 4.9	31.7 ± 2.0	29.9 ± 1.4	31.4 ± 1.1	15.5 ± 1.6	19.5 ± 0.8	0.51	0.81
		400	96.2 ± 0.2	55.3 ± 1.2	48.4 ± 0.3	15.7 ± 0.3	14.4 ± 0.9	17.7 ± 0.3	0.24	0.83
20	4000	300	98.2 ± 0.1	50.8 ± 0.1	29.8 ± 0.0	33.1 ± 0.0	16.3 ± 0.1	19.1 ± 0.1	0.53	0.93
		350	99.7 ± 0.1	57.0 ± 0.2	31.2 ± 0.4	36.1 ± 0.6	17.6 ± 0.4	14.9 ± 0.2	0.54	0.90
		400	99.2 ± 0.1	62.2 ± 0.6	48.0 ± 1.6	25.2 ± 1.6	12.2 ± 0.6	13.8 ± 0.1	0.34	0.91
	6000	300	90.5 ± 0.3	42.6 ± 0.2	26.4 ± 0.3	31.9 ± 0.2	15.6 ± 0.5	21.0 ± 0.0	0.55	0.93
		350	99.6 ± 0.1	53.0 ± 0.1	35.5 ± 0.2	33.8 ± 0.2	11.8 ± 0.4	18.7 ± 0.0	0.49	0.87
		400	99.1 ± 0.0	60.3 ± 0.1	48.7 ± 0.7	26.5 ± 0.6	8.5 ± 1.0	15.5 ± 0.1	0.35	0.87
	8000	300	97.2 ± 0.2	48.8 ± 0.2	30.2 ± 0.4	29.8 ± 0.8	17.7 ± 0.4	19.6 ± 0.0	0.50	0.89
		350	99.3 ± 0.1	53.7 ± 0.3	33.7 ± 0.8	32.6 ± 1.4	15.6 ± 1.8	17.5 ± 0.4	0.49	0.86
		400	98.5 ± 0.1	58.7 ± 0.3	52.6 ± 1.3	22.4 ± 0.9	7.8 ± 1.7	15.6 ± 0.1	0.30	0.86

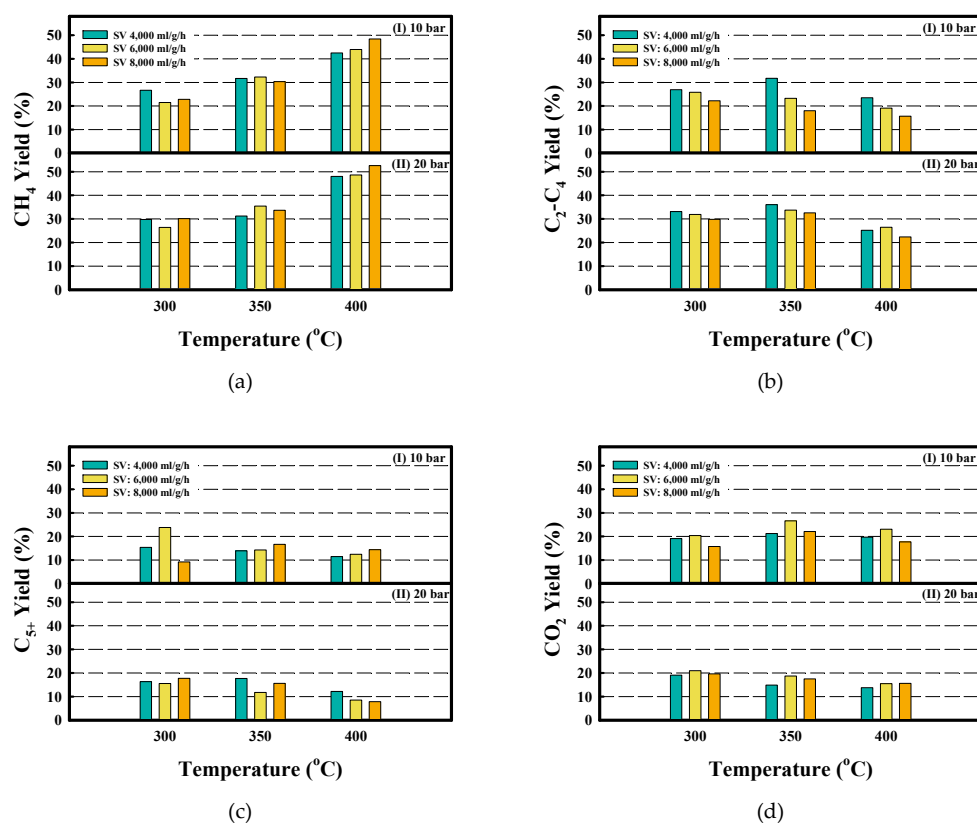


Figure 4. The initial yield of (a) CH₄, (b) C₂–C₄, (c) C₅₊ and (d) CO₂ over the FT catalyst (5Co-15Fe/ γ -Al₂O₃) at different space velocity as a function of reaction temperature at (I) 10 bar and (II) 20 bar.

Figure 4 shows the initial product yields for (a) CH₄, (b) C₂–C₄, (c) C₅₊ and (d) CO₂ under high CO conversion conditions (≥ 300 °C). The effects of reaction parameters such as space velocity, reaction pressure and temperature on product distribution are strongly dependent on the secondary reactions of primary products including hydrogenation, reinsertion, hydrogenolysis, and isomerization [19,20]. It is well known that CH₄ increases and C₅₊ hydrocarbons decreases with increasing space velocity under typical FTS conditions. In addition, an increase in reaction temperature shifts the hydrocarbon distribution towards light hydrocarbon products, whereas an increase in reaction pressure shifts the hydrocarbon distribution to heavier products in typical FTS reaction [19]. As shown in Figure 4a, CH₄ yield increases with the increase in reaction temperature under all reaction pressures and space velocities. In contrast to typical FTS conditions, improved CH₄ yield at high reaction pressure (20 bar) indicates that the higher reaction pressure is favorable for secondary CO₂ methanation reaction, as discussed below in Figure 4d [21–24]. In addition, space velocity did not affect methane yield at relatively low temperature (300 and 350 °C), whereas CH₄ yield increases with the increase in space velocity at 400 °C. As shown in Figure 4b, C₂–C₄ yield reached the highest values at 300 or 350 °C, and then decreased at higher reaction temperatures. Furthermore, reaction pressure enhanced C₂–C₄ yield, and space velocity is inversely proportional to C₂–C₄ yield. In the case of C₅₊ hydrocarbon yield, although it is difficult to confirm the effects of reaction parameters, C₅₊ yield decreased with the increase in reaction pressure and temperature (Figure 4c). As shown in Figure 4d, CO₂ yield exhibited almost the same values (ca. 20%) at reaction temperatures between 350 and 400 °C. This is due to the fact that the increase in CO₂ production with increasing CO conversion can mainly be attributed to increased water gas-shift reaction (WGS, CO + H₂O \leftrightarrow CO₂ + H₂) at high water partial pressures [11,25]. At 20 bar, however, it is notable that CO₂ yield decreases with the increase in reaction temperature, despite almost 100% CO conversion at all temperatures. These results show that higher reaction pressure and temperature are favorable conditions for secondary CO₂ methanation reaction.

Figure 5 shows the yield of light hydrocarbons in C_1 – C_4 range and ratio of C_2 – C_4 to C_1 – C_4 yield under different reaction parameters, such as space velocity, reaction temperature and pressure. At 10 bar, sum of CH_4 and C_2 – C_4 yield increased (45–53 to 63–66%), and ratio of C_2 – C_4 to C_1 – C_4 yield decreased (0.5–0.55 to 0.25–0.35) with the increase in reaction temperature between 300 to 400 °C, as shown in Figure 5a. The sum of CH_4 and C_2 – C_4 yield decreased from 53 to 45% at 300 °C, but these values did not change a lot at higher reaction temperature (350 and 400 °C) with an increase in space velocity. In addition, the ratio of C_2 – C_4 to C_1 – C_4 yield decreased from 0.35 to 0.25 at 400 °C, but its value remained constant (ca. 0.5–0.55) at lower temperature (300 and 350 °C). At 20 bar, the sum of CH_4 and C_2 – C_4 yield increased (58–63% to 73–75%), and the ratio of C_2 – C_4 to C_1 – C_4 yield decreased (0.49–0.55 to 0.30–0.35), with the increase in reaction temperature between 300 to 400 °C, as shown in Figure 5b. The sum of CH_4 and C_2 – C_4 yield remained constant at all reaction temperatures between 300 and 400 °C. In addition, the ratio of C_2 – C_4 to C_1 – C_4 yield decreased from 0.35 to 0.30 at 400 °C, but its value remained constant (ca. 0.5–0.55) at lower temperature (300 and 350 °C). Overall, the yield of light hydrocarbons in C_1 – C_4 range increased with increasing in reaction temperature between 300 to 400 °C, because CH_4 yield increases dramatically and C_2 – C_4 yield decreases slightly, resulting in reduction of $(C_2-C_4)/(C_1-C_4)$ ratio. With increasing in space velocity, on the other hand, the sum of CH_4 and C_2 – C_4 yield and $(C_2-C_4)/(C_1-C_4)$ ratio decreased slightly. Furthermore, high reaction pressure enhanced the light hydrocarbon (C_1 – C_4) yield and the $(C_2-C_4)/(C_1-C_4)$ ratio. At both 10 and 20 bar, a space velocity of 4000 mL/g/h and 350 °C are considered to be appropriate conditions for high calorific methanation, since the 5Co-15Fe/ γ - Al_2O_3 catalyst exhibit the highest light hydrocarbon (CH_4 and C_2 – C_4) yield and $(C_2-C_4)/(C_1-C_4)$, respectively.

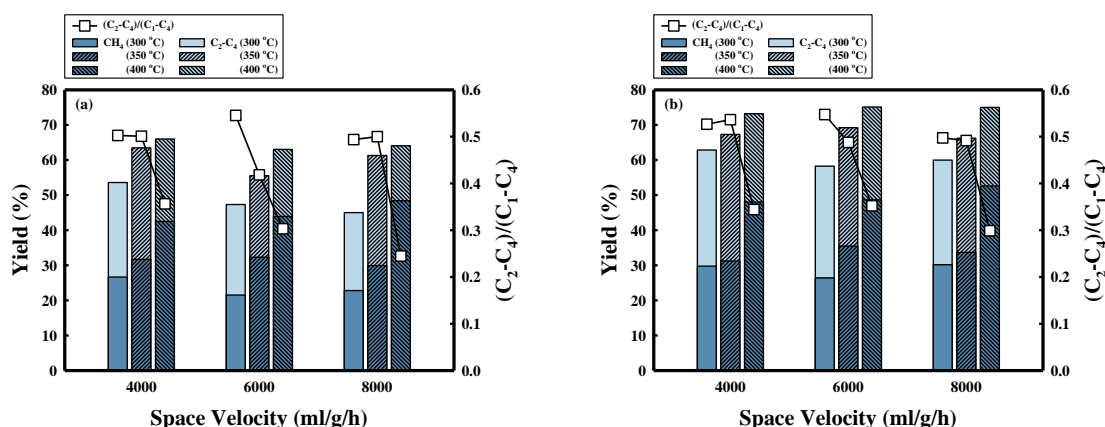


Figure 5. C_1 – C_4 yield and $(C_2-C_4)/(C_1-C_4)$ ratio of the FT catalyst (5Co-15Fe/ γ - Al_2O_3) as a function of space velocity at (a) 10 bar and (b) 20 bar

Figure 6 shows the paraffin ratio ($P/(P+O)$) with different reaction parameters, such as H_2/CO ratio, space velocity, reaction pressure and temperature, where P and O represent the yields of paraffins and olefins in the C_2 – C_4 range, respectively. As shown in Figure 6a, the paraffin ratio increased with increasing H_2/CO ratio at a space velocity of 6000 mL/g/h, although this effect is not noticeable at H_2/CO ratios above 2.0, due to the adjustment of H_2/CO ratio by WGS conditions [11,25]. In addition, it was found that the paraffin ratio showed a positive correlation with CO conversion. The fact that the paraffin ratio increases with the CO conversion suggests that increasing the H_2/CO ratio and temperatures leads to a second hydrogenation of the olefins into paraffin and an increase of the CO conversion. As shown in Figure 6b, space velocity, reaction pressure and temperature have little effect on paraffin ratio at H_2/CO ratio of 3.0, but CO conversion is strongly dependent on reaction temperature. Furthermore, it is found that a higher reaction pressure (20 bar) improved the CO conversion above a reaction temperature of 300 °C, because higher reaction pressure enhanced hydrogen adsorption on support of the catalyst and improved second hydrogenation [19].

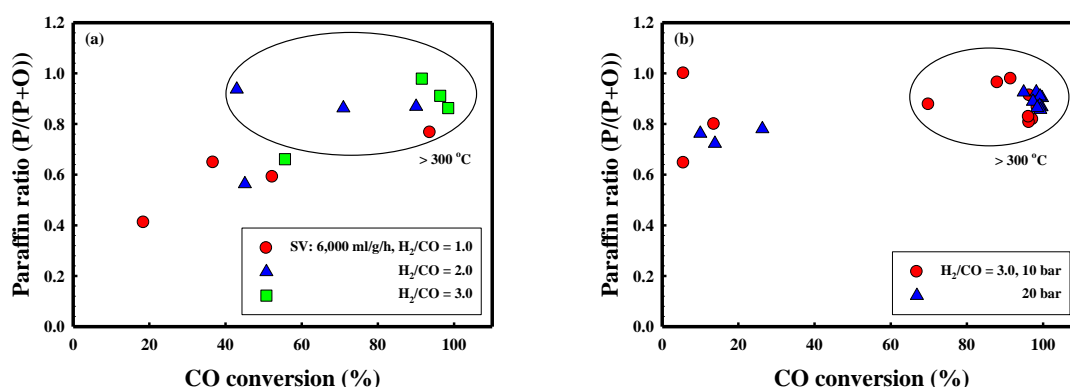


Figure 6. Paraffin ratio of the FT catalyst (5Co-15Fe/ γ -Al₂O₃) as a function of CO conversion at different operating conditions: (a) effect of H₂/CO ratio at SV of 6000 ml/g/h, and (b) effect of reaction pressure at H₂/CO ratio of 3.0.

Table 3 shows the comparison of the 5Co-15Fe/ γ -Al₂O₃ catalyst under optimum conditions with different catalysts published in other papers. As listed in Table 3, Co-Mn-Ru catalysts showed high CO conversion and CH₄ yield, but relatively low C₂₊ hydrocarbon yield, compared to Fe-based catalysts [7,8]. Lee et al. [7] reported that Mn promoter in cobalt catalysts acted as a Lewis acid, which increased the carbon chain growth and C₂₊ hydrocarbon yield, but suppressed CO conversion. Ru promoter, one of the noble metals, provided the catalyst with hydrogen spillover ability, enhancing the reducibility of the cobalt site and CO conversion, but decreasing the C₂₊ hydrocarbon yield. In addition, Ru promoters were substituted to save cost for the catalysts, and 20Co-16Mn/ γ -Al₂O₃ catalyst reduced at 700 °C for 1 h showed similar reactivity to 10Co-6Mn-2.5Ru/ γ -Al₂O₃ catalyst reduced at 400 °C for 1 h. The Fe-based bulk catalysts promoted by Cu and Zn showed high CO conversion and C₂–C₄ yield, but low paraffin ratio and high byproduct yield (C₅₊ and CO₂) [8,9]. On the other hand, the FT catalyst (5Co-15Fe/ γ -Al₂O₃) affords high CO conversion (99.7%), high light paraffinic hydrocarbon yield (31.2% CH₄ and 36.1% C₂–C₄), and low byproduct formation (C₅₊ and CO₂) under optimum conditions (SV: 4000 mL/g/h, T: 350 °C and P: 20 bar).

Table 3. Comparison of catalytic performance of FT catalyst (5Co-15Fe/ γ -Al₂O₃) with different catalysts published in other papers.

Catalysts	H ₂ /CO	Reaction Condition	CO Conv. (%)	Yield				P/(P+O)	Ref
				CH ₄	C ₂ –C ₄	C ₅₊	CO ₂		
5Co-15Fe/ γ -Al ₂ O ₃	3.0	SV: 6000 ml/g/h, 300 °C, 10 bar	91.5	21.5	25.8	23.8	20.4	0.98	This study
	3.0	SV: 4000 ml/g/h, 350 °C, 20 bar	99.7	31.2	36.1	17.6	14.9	0.90	This study
10Co-6Mn-2Ru/ γ -Al ₂ O ₃ ^a	3.0	SV: 6000 ml/g/h, 300 °C, 10 bar	99.7	60.6	24.5	4.8	10.9	0.96	[8]
10Co-6Mn-2.5Ru/ γ -Al ₂ O ₃ ^b	3.0	SV: 6000 ml/g/h, 250 °C, 10 bar	100.0	53.0	23.0	8.6	n/a [§]	n/a [§]	[7]
20Co-16Mn/ γ -Al ₂ O ₃ ^c	3.0	SV: 6000 ml/g/h, 250 °C, 10 bar	92.0	53.0	24.0	5.8	n/a [§]	n/a [§]	[7]
FC15 ^d	3.0	SV: 6000 ml/g/h, 300 °C, 10 bar	97.5	21.5	35.7	12.9	27.4	0.58	[9]
FZ5 ^e	3.0	SV: 6000 ml/g/h, 300 °C, 10 bar	89.9	19.1	35.3	24.1	24.1	0.76	[8]
FZ10 ^f	3.0	SV: 6000 ml/g/h, 300 °C, 10 bar	98.2	23.7	40.0	12.7	21.9	0.70	[8]

^a 10 wt.% Co, 6 wt.% Mn, and 2 wt.% Ru, reduced at for 400 °C for 1h. ^b 10 wt.% Co, 6 wt.% Mn, and 2.5 wt.% Ru, reduced at for 400 °C for 1h. ^c 20 wt.% Co, 16 wt.% Mn, reduced at for 700 °C for 1h. ^d Fe/Cu atomic ratio = 15, reduced at 500 °C for 1 h. ^e Fe/Zn atomic ratio = 5, reduced at 500 °C for 1 h. ^f Fe/Zn atomic ratio = 10, carburized at 500 °C for 1 h. [§] n/a: Not applicable.

3. Materials and Methods

3.1. Catalyst Synthesis

The bimetallic Co-Fe catalyst was synthesized by wet impregnation of γ -alumina (Sigma-Aldrich, St. Louis, MO, USA) with $\text{Co}(\text{NO}_3)_2 \cdot 6\text{H}_2\text{O}$ (Sigma-Aldrich, St. Louis, MO, USA) and $\text{Fe}(\text{NO}_3)_3 \cdot 9\text{H}_2\text{O}$ (Sigma-Aldrich, St. Louis, MO, USA) according to the same method as our previous papers [11,12]. During the impregnation procedure of the FT catalyst (5Co-15Fe/ γ - Al_2O_3), γ - Al_2O_3 was added to an anhydrous ethanol solution containing cobalt and iron nitrates. The weight percentages of the cobalt and iron metal based on the catalyst were 5% and 10%, respectively. After stirring for 24 h, the solvent was vaporized in a rotary evaporator at 40–60 °C. The samples were dried at 120 °C for 12 h, and subsequently calcined at 400 °C for 8 h.

3.2. Characterization

The metal contents in FT catalyst were measured using inductively coupled plasma optical emission spectroscopy (ICP-OES; Perkin-Elmer, Waltham, MA, USA). Nitrogen adsorption-desorption isotherms at -196 °C were measured using a Micrometrics ASAP 2020 instrument (Norcross, GA, USA) to acquire the textural properties of the materials. Average pore size were measured following the Barrett-Joyner-Halenda (BJH) method. The crystal structure of the FT catalyst was analyzed via X-ray diffraction (XRD; PANalytical, Amsterdam, Netherlands) using a Cu K α radiation source at the Korea Basic Science Institute in Daegu. Crystallite sizes of metal phase were calculated using the Scherer equation.

3.3. Activity Tests

Prior to the reaction, the catalysts (0.5 g) were placed in a fixed-bed stainless steel reactor (1/2 inch I.D.) and reduced with a 10 vol% H_2/N_2 gas mixture at 500 °C for 1 h. Then, the gas stream (H_2 , CO , N_2) was fed to the reactor at a different total gas flow (33, 50 and 60 mL/min); N_2 gas was used as an internal standard in the feed gas. The reactor was pressurized to 10 or 20 bar with the feed gas stream using a back-pressure regulator at constant pressure and heated to 200 °C. Then, the temperature was increased to 250, 300, 350, or 400 °C, and maintained during the FT reaction. All volumetric gas flows were measured at standard temperature and pressure (S.T.P). To prevent the condensation of water vapor and hydrocarbons, the inlet and outlet lines of the reactor were maintained at temperatures above 250 °C, and the liquid and wax products were collected in a cold trap (0 °C) before injection of the gas into the reactor and GC column. The outlet gases were analyzed using a gas chromatograph (Agilent 6890; Agilent, Santa Clara, CA, USA) equipped with both a thermal conductivity detector (TCD), and a flame ionization detector (FID). A packed column (Carboxen 1000; Bellefonte, PA, USA) was connected to the TCD to analyze the CO , H_2 , N_2 , and CO_2 gases, and a capillary column (GS Gas Pro; Agilent, Santa Clara, CA, USA) was connected to the FID to analyze the hydrocarbon gases.

CO conversion, selectivity and yield for each product were calculated using Equations (1)–(4).

$$\text{CO conversion (carbon mole \%)} = \left(1 - \frac{\text{CO in the product gas (mol/min)}}{\text{CO in the feed gas (mol/min)}}\right) \times 100 \quad (1)$$

$$\begin{aligned} &\text{Selectivity for hydrocarbons with carbon number } n \text{ (carbon mole \%)} \\ &= \frac{n \times C_n \text{ hydrocarbon in the product gas (mol/min)}}{(\text{total carbon-unreacted CO}) \text{ in the product gas (mol/min)}} \times 100 \end{aligned} \quad (2)$$

$$\begin{aligned} &\text{Selectivity for carbon dioxide (carbon mole \%)} \\ &= \frac{\text{CO}_2 \text{ in the product gas (mol/min)}}{(\text{total carbon-unreacted CO}) \text{ in the product gas (mol/min)}} \times 100 \end{aligned} \quad (3)$$

$$\text{Yield for hydrocarbons and carbon dioxide} = \frac{\text{CO conversion} \times \text{Selectivity}}{100} \quad (4)$$

4. Conclusions

At present, few studies have made an effort to produce mixing gases consisting of paraffinic C₂–C₄ hydrocarbons into SNG for power generation. In this study, bimetallic Co-Fe catalysts supported on γ -alumina were developed, and the effects of operating parameters such as space velocity, reaction pressure and temperature on catalytic performance were elucidated for the production of light paraffin hydrocarbon yield (C₂–C₄ range) with high paraffin ratio, as well as reduction of byproduct formation (C₅₊ and CO₂). It was found that CO conversion increases with a decrease in space velocity, and with an increase in reaction pressure and temperature. CH₄ yield increases and C₂₊ yield decreases with increasing reaction temperature at all reaction pressures and space velocities. In addition, improved CH₄ yield at higher reaction pressure (20 bar) implies that higher reaction pressure is a favorable condition for secondary CO₂ methanation reaction. While paraffin ratio shows a positive correlation with the CO conversion according to increasing H₂/CO ratio, reaction pressure and temperature have little effect on paraffin ratio at a H₂/CO ratio of 3.0. Based on these results, the optimum conditions were determined to be H₂/CO of 3.0, space velocity of 4000 mL/g/h, reaction pressure of 20 bar, and temperature of 300 °C, and the FT catalyst (5Co-15Fe/ γ -Al₂O₃) affords a high light hydrocarbon yield (31.2 % CH₄, and 36.1 % C₂–C₄) with high paraffin ratio (0.90). Based on these results, the bimetallic Co-Fe catalysts can be used for production of high paraffinic light hydrocarbons.

Supplementary Materials: The following are available online at <http://www.mdpi.com/2073-4344/9/9/779/s1>, Figure S1: XRD patterns of (I) fresh and (II) reduced monometallic and bimetallic Co-Fe catalysts; (●) Co₃O₄, (▲) CoO, (△) Co metal, (◆) Fe₂O₃, (■) Fe₃O₄, and (□) Fe metal; Figure S2. H₂-TPR profiles of the monometallic and bimetallic catalysts supported on γ -alumina: (a) 20Co/ γ -Al₂O₃, (b) 15Co-5Fe/ γ -Al₂O₃, (c) 10Co-10Fe/ γ -Al₂O₃, (d) 5Co-15Fe/ γ -Al₂O₃, and (e) 20Fe/ γ -Al₂O₃ (5 °C/min, pure hydrogen); Figure S3: CO conversion and hydrocarbon distribution of the monometallic and bimetallic catalysts supported on γ -alumina: 20Co/ γ -Al₂O₃, 15Co-5Fe/ γ -Al₂O₃, 10Co-10Fe/ γ -Al₂O₃, 5Co-15Fe/ γ -Al₂O₃, and 20Fe/ γ -Al₂O₃ at H₂/CO ratio = 3.0, 300 °C, and 10 bar.

Author Contributions: Conceptualization, S.B.J., T.Y.K., S.-H.K. and J.W.K.; Data curation, S.B.J., T.Y.K., C.H.L. and J.H.W.; Formal analysis, T.Y.K., C.H.L., J.H.W. and H.J.C.; Investigation, S.B.J. and T.Y.K.; Project administration, S.C.L. and J.C.K.; Supervision, S.C.L. and J.C.K.; Writing—original draft, S.B.J.; Writing—review & editing, S.B.J. and T.Y.K.

Funding: This research was funded by the Korea Institute of Energy Technology Evaluation and Planning (KETEP) and the Ministry of Trade, Industry & Energy (MOTIE) of the Republic of Korea (No.20173010050110 and the Basic Science Research Program through the National Research Foundation of Korea (NRF) funded by the Ministry of Science, ICT & Future Planning (No.2017R1A2B4008275).

Acknowledgments: This work was supported by the Korea Institute of Energy Technology Evaluation and Planning (KETEP) and the Ministry of Trade, Industry & Energy (MOTIE) of the Republic of Korea. (No.20173010050110). This research was also supported by the Basic Science Research Program through the National Research Foundation of Korea (NRF) funded by the Ministry of Science, ICT & Future Planning (No.2017R1A2B4008275).

Conflicts of Interest: The authors declare no conflict of interest.

References

1. Zhao, B.; Chen, Z.; Chen, Y.; Ma, X. Syngas methanation over Ni/SiO₂ catalyst prepared by ammonia-assisted impregnation. *Int. J. Hydrog. Energy* **2017**, *42*, 27073–27083. [CrossRef]
2. Hwang, S.; Lee, J.; Hong, U.G.; Gil Seo, J.; Jung, J.C.; Koh, D.J.; Lim, H.; Byun, C.; Song, I.K. Methane production from carbon monoxide and hydrogen over nickel–alumina xerogel catalyst: Effect of nickel content. *J. Ind. Eng. Chem.* **2011**, *17*, 154–157. [CrossRef]
3. Gao, J.; Jia, C.; Li, J.; Zhang, M.; Gu, F.; Xu, G.; Zhong, Z.; Su, F. Ni/Al₂O₃ catalysts for CO methanation: Effect of Al₂O₃ supports calcined at different temperatures. *J. Energy Chem.* **2013**, *22*, 919–927. [CrossRef]
4. Kopyscinski, J.; Schildhauer, T.J.; Biollaz, S.M. Production of synthetic natural gas (SNG) from coal and dry biomass—A technology review from 1950 to 2009. *Fuel* **2010**, *89*, 1763–1783. [CrossRef]
5. Liu, Y.; Zhu, L.; Wang, X.; Yin, S.; Leng, F.; Zhang, F.; Lin, H.; Wang, S. Catalytic methanation of syngas over Ni-based catalysts with different supports. *Chin. J. Chem. Eng.* **2017**, *25*, 602–608. [CrossRef]

6. Inui, T.; Sakamoto, A.; Takeguchi, T.; Ishigaki, Y. Synthesis of highly calorific gaseous fuel from syngas on cobalt-manganese-ruthenium composite catalysts. *Ind. Eng. Chem. Res.* **1989**, *28*, 427–431. [[CrossRef](#)]
7. Lee, Y.H.; Kim, H.; Choi, H.S.; Lee, D.-W.; Lee, K.-Y. Co-Mn-Ru/Al₂O₃ catalyst for the production of high-calorific synthetic natural gas. *Korean J. Chem. Eng.* **2015**, *32*, 2220–2226. [[CrossRef](#)]
8. Lee, Y.H.; Lee, D.-W.; Kim, H.; Choi, H.S.; Lee, K.-Y. Fe–Zn catalysts for the production of high-calorie synthetic natural gas. *Fuel* **2015**, *159*, 259–268. [[CrossRef](#)]
9. Lee, Y.H.; Lee, D.-W.; Lee, K.-Y. Production of high-calorie synthetic natural gas using copper-impregnated iron catalysts. *J. Mol. Catal. A Chem.* **2016**, *425*, 190–198. [[CrossRef](#)]
10. Lee, Y.H.; Lee, K.-Y. Effect of surface composition of Fe catalyst on the activity for the production of high-calorie synthetic natural gas (SNG). *Korean J. Chem. Eng.* **2017**, *34*, 320–327. [[CrossRef](#)]
11. Jo, S.B.; Chae, H.J.; Kim, T.Y.; Lee, C.H.; Oh, J.U.; Kang, S.-H.; Kim, J.W.; Jeong, M.; Lee, S.C.; Kim, J.C. Selective CO hydrogenation over bimetallic Co-Fe catalysts for the production of light paraffin hydrocarbons (C₂–C₄): Effect of H₂/CO ratio and reaction temperature. *Catal. Commun.* **2018**, *117*, 74–78. [[CrossRef](#)]
12. Jo, S.B.; Kim, T.Y.; Lee, C.H.; Kang, S.-H.; Kim, J.W.; Jeong, M.; Lee, S.C.; Kim, J.C. Hybrid catalysts in a double-layered bed reactor for the production of C₂–C₄ paraffin hydrocarbons. *Catal. Commun.* **2019**, *127*, 29–33. [[CrossRef](#)]
13. Lee, J.; Kang, S. Formation behaviours of mixed gas hydrates including olefin compounds. *Chem. Eng. Trans.* **2013**, *32*, 1921–1926.
14. Griboval-Constant, A.; Butel, A.; Ordonsky, V.V.; Chernavskii, P.A.; Khodakov, A.; Khodakov, A. Cobalt and iron species in alumina supported bimetallic catalysts for Fischer–Tropsch reaction. *Appl. Catal. A Gen.* **2014**, *481*, 116–126. [[CrossRef](#)]
15. Lögdberg, S.; Tristantini, D.; Borg, Ø.; Ilver, L.; Gevert, B.; Järås, S.; Blekkan, E.A.; Holmén, A. Hydrocarbon production via Fischer–Tropsch synthesis from H₂-poor syngas over different Fe-Co/γ-Al₂O₃ bimetallic catalysts. *Appl. Catal. B Environ.* **2009**, *89*, 167–182. [[CrossRef](#)]
16. Rytter, E.; Holmen, A. Deactivation and Regeneration of Commercial Type Fischer-Tropsch Co-Catalysts—A Mini-Review. *Catalysts* **2015**, *5*, 478–499. [[CrossRef](#)]
17. Gao, J.; Gu, F.; Zhong, Z.; Liu, Q.; Su, F. Recent advances in methanation catalysts for the production of synthetic natural gas. *RSC Adv.* **2015**, *5*, 22759–22776. [[CrossRef](#)]
18. Meng, F.; Li, X.; Lv, X.; Li, Z. Co hydrogenation combined with water-gas-shift reaction for synthetic natural gas production: A thermodynamic and experimental study. *Int. J. Coal Sci. Technol.* **2018**, *5*, 439–451. [[CrossRef](#)]
19. Yang, J.; Ma, W.; Chen, D.; Holmén, A.; Davis, B.H. Fischer–Tropsch synthesis: A review of the effect of CO conversion on methane selectivity. *Appl. Catal. A Gen.* **2014**, *470*, 250–260. [[CrossRef](#)]
20. Novak, S. Secondary effects in the Fischer-Tropsch synthesis. *J. Catal.* **1982**, *77*, 141–151. [[CrossRef](#)]
21. Frontera, P.; Macario, A.; Ferraro, M.; Antonucci, P. Supported Catalysts for CO₂ Methanation: A Review. *Catalysts* **2017**, *7*, 59. [[CrossRef](#)]
22. Kirchner, J.; Anolleck, J.K.; Lösch, H.; Kureti, S. Methanation of CO₂ on iron based catalysts. *Appl. Catal. B Environ.* **2018**, *223*, 47–59. [[CrossRef](#)]
23. Le, T.A.; Kim, M.S.; Lee, S.H.; Kim, T.W.; Park, E.D. CO and CO₂ methanation over supported Ni catalysts. *Catal. Today* **2017**, *293*, 89–96. [[CrossRef](#)]
24. Stangeland, K.; Kalai, D.; Li, H.; Yu, Z. CO₂ Methanation: The Effect of Catalysts and Reaction Conditions. *Energy Procedia* **2017**, *105*, 2022–2027. [[CrossRef](#)]
25. Galvis, H.M.T.; De Jong, K.P. Catalysts for Production of Lower Olefins from Synthesis Gas: A Review. *ACS Catal.* **2013**, *3*, 2130–2149. [[CrossRef](#)]

